

Probing Non-Standard Couplings of Neutrinos at the Borexino Detector

Zurab Berezhiani^{a,b,1}, R. S. Raghavan^{c,2} and Anna Rossi^{d,3}

^a *Dipartimento di Fisica, Università di L'Aquila, I-67010 Coppito, AQ, and
INFN, Laboratori Nazionali del Gran Sasso, I-67010 Assergi, AQ, Italy*

^b *The Andronikashvili Institute of Physics, Georgian Academy of Sciences,
380077 Tbilisi, Georgia*

^c *Bell Laboratories, Lucent Technologies, Murray Hill, New Jersey 07974.*

^d *Dipartimento di Fisica, Università di Padova and INFN Sezione di Padova,
I-35131 Padova, Italy.*

Abstract

The present experimental status does not exclude weak-strength non-standard interactions of neutrinos with electrons. These interactions can be revealed in solar neutrino experiments. Our discussion covers several aspects related to this issue. First, we perform an analysis of the Super Kamiokande and SNO data to investigate their sensitivity to such interactions. Second, we suggest that the Borexino detector provides good signatures for these non-standard interactions. Indeed, in Borexino the shape of the recoil electron spectrum essentially does not depend on the solar neutrino conversion details, since most of the signal comes from the mono-energetic ${}^7\text{Be}$ neutrinos. Therefore, the conversion of solar ν_e into a state composed of a nearly equal mixture of ν_μ and ν_τ , as is indicated by the atmospheric neutrino data, offers the chance to detect extra interactions of ν_τ in the measurement of the recoil electron spectrum in the $\nu e \rightarrow \nu e$ scattering. In addition, we perform the same analysis assuming non-standard interactions for ν_e .

¹ E-mail address: berezhiani@fe.infn.it

² E-mail address: raju@physics.bell-labs.com

³ E-mail address: arossi@pd.infn.it

1 Introduction

There is a compelling evidence that neutrinos do oscillate and then they may be mixed and massive. In particular, the atmospheric neutrino anomaly (ANA) can be interpreted in terms of $\nu_\mu \rightarrow \nu_\tau$ oscillations with $\delta m_{atm}^2 \sim (1.6 \div 4) \times 10^{-3} \text{eV}^2$ and $\sin^2 2\theta > 0.88$ at 68% CL [1]. As for the solar neutrino anomaly (SNA), the interpretation is less clear and many neutrino conversion mechanisms can be invoked [2]. Very recently, the SNO collaboration has published their first results which unambiguously confirm the solar neutrino suppression [3]. In particular, the comparison between the charged-current (CC) measurements performed by SNO and the Super Kamiokande data may disfavour solutions involving the ν_e conversion into a sterile state ν_s [3, 4].

At present, in the context of three (active) neutrino states the following paradigm for the neutrino mixing and mass pattern arises.

- (i) ν_μ and ν_τ are nearly maximally mixed, $\theta_{23} \sim 45^\circ$ and $\delta m_{23}^2 \equiv \delta m_{atm}^2 \sim 3 \times 10^{-3} \text{eV}^2$: the oscillation channel responsible for the ANA is mostly $\nu_\mu \rightarrow \nu_\tau$;
- (ii) the conversion $\nu_e \rightarrow \nu_\mu$ is responsible for the SNA and these two states can be either tinily or strongly mixed, $\theta_{12} \sim 2^\circ$ or $\theta_{12} \gtrsim 25^\circ$ depending on the specific solution adopted, with a corresponding δm_{sol}^2 ranging from 10^{-12} up to 10^{-4}eV^2 [2, 4];
- (iii) the combined accommodation of the atmospheric and solar neutrino data points to a very small mixing angle between ν_e and ν_τ , $\theta_{13} \lesssim 0.1$. Moreover, this result is in agreement with the data of the CHOOZ experiment [5].

In conclusion, the lepton mixing matrix V connecting the neutrino flavour eigenstates (ν_e, ν_μ, ν_τ) with the mass eigenstates (ν_1, ν_2, ν_3), *viz.* $\nu_\alpha = V_{\alpha i} \nu_i$, can be parameterised as:

$$V = \begin{pmatrix} c_{12} & s_{12} & 0 \\ -s_{12}c_{23} & c_{12}c_{23} & s_{23} \\ s_{12}s_{23} & -c_{12}s_{23} & c_{23} \end{pmatrix}, \quad (\alpha = e, \mu, \tau, \quad i = 1, 2, 3), \quad (1)$$

where $s_{ij} = \sin \theta_{ij}$, $c_{ij} = \cos \theta_{ij}$ and $s_{13} = 0$ has been assumed. Therefore the electron neutrino is mixed with a θ_{23} -combination of muon and tau neutrino, $\nu_a = (c_{23} \cdot \nu_\mu - s_{23} \cdot \nu_\tau)$. In the picture sketched above, the SNA oscillation parameters in fact refer to the system $\nu_e - \nu_a$. As this means that solar neutrinos are converted into a nearly equal mixture of ν_μ and ν_τ , the Sun appears as a copious source of *tau neutrinos*. In the framework of the Standard Model (SM) interactions the flavour states ν_μ and ν_τ are indistinguishable as far as the neutral current (NC) interactions are concerned and therefore, for example, the ν_a - e elastic-scattering cross section is not sensitive to the mixing angle θ_{23} , that is to the flavour content of ν_a .

Alternatively, there exists the possibility that the solar neutrino problem be explained in terms of a conversion into a sterile state ν_s , i.e. a singlet with respect to the SM. This case has been extensively analysed in literature. As mentioned, recently in view of the SNO data all the solutions involving the sterile conversion are less favoured as compared to those involving the analogous active conversion.

Here we would like to put forward the possibility to ‘identify’ the ν_τ in solar neutrino elastic scattering experiments like Borexino that is to say to test the large 2-3 mixing angle required by atmospheric neutrinos, by assuming the tau neutrino to have non-standard (NS)

weak-strength interactions with the electron. Some time ago [6] we discussed the impact of extra ν_τ interactions with electrons on the detection cross section in the context of the neutrino long wavelength oscillation as a solution to the SNA. In a different perspective, we should also recall that non-standard flavour changing neutrino interactions have been invoked long ago to explain the SNA [7, 6, 8, 9]. (For a more recent analysis, see for example [10].) As a matter of fact neutrino NS interactions would also affect the neutrino survival probability of mechanisms such as the Mikheyev-Smirnov-Wolfenstein (MSW) resonant conversion in matter [11] or the neutrino decay in matter [12]. As for the muon neutrino, ν_μ , the accelerator constraints are severe and thus in the following it is assumed to have only SM interactions [9]. On the contrary, as regards the electron neutrino ν_e the existing laboratory bounds from low-energy ν_e - e scattering experiments are weak. For the ν_τ there are no direct limits from low-energy experiments. Indeed, the constraints on non-standard interactions rather apply to the ν_τ $SU(2)_W$ -partner, the tau lepton. However, non-standard interactions of neutrinos with electrons can be constrained at e^+e^- colliders via the channel $e^+e^- \rightarrow \nu\bar{\nu}\gamma$, as recently suggested in [13]. The result of that analysis still allows some relevant range for neutrino NS interactions that therefore could be tested by a solar neutrino experiment like Borexino, as we shall demonstrate.

Here, first we study the impact of neutrino NS interactions on the present solar neutrino phenomenology. Neutrino extra interactions with electrons can affect the detection reaction $\nu-e \rightarrow \nu-e$ used by Super Kamiokande. Therefore it is necessary to explore the features that may emerge in this case when comparing the Super Kamiokande and SNO data.

It is well-known that the measurement of the neutrino energy spectrum in solar neutrino experiments may be used to discriminate the several SNA solutions as it does not depend on the solar-model theory. In general the deformation of the energy spectrum is expected to arise from the energy dependence of the neutrino survival probability $P(E)$ (E is the neutrino energy). The effect we would like to study would then be superimposed to that induced by the energy dependence of P . Notice, however, that the effect induced by $P(E)$ on the energy spectrum can nicely be ‘factorised out’ in the case of monochromatic neutrinos, such as the solar ${}^7\text{Be}$ ($E = 0.862$ MeV) and pep ($E = 1.414$ MeV) neutrinos and thus the specific deformation might only be attributed to the ν non-standard interactions involved in the detection reaction $\nu - e \rightarrow \nu - e$. Therefore, the capability of Borexino experiment is unique in that it could be sensitive to this novel spectral distortion induced by NS ν interactions.

We think that now, in view of the robust evidence of a large mixing angle in the $\nu_\mu - \nu_\tau$ system provided by Super-Kamiokande atmospheric data, it is worthwhile to reconsider and stress further the impact of ν_τ extra interactions on the differential ν - e cross section. The observation of such an effect would simultaneously provide the signature of novel interactions of neutrinos and would be a further proof of the large mixing angle θ_{23} i.e. a test of the atmospheric neutrino oscillations. This experimental evidence would be complementary to that achieved by Super-Kamiokande and DONUT experiments which both claim to have observed charged current ν_τ events [1, 14].

The content of this paper is organized as follows. In Sec. 2 we present the effective Lagrangian describing the neutrino NS interactions with electrons and we recall the present limits on non-standard interactions extracted by accelerator experiments. In Sec. 2.1 we discuss the modification induced on the differential ν - e cross section, relevant for solar neutrino experiments, by neutrino NS interactions. In Sec. 3 we consider the relevance of NS interactions in the comparison between SNO CC data and Super Kamiokande data. We shall consider both

cases of active-sterile conversion (Sec. 3.1) and pure active conversion assuming ν_τ and ν_e to have neutrino NS interactions (Sec. 3.2). We will see that the two solar neutrino experiments cannot constrain further the strength of the new interactions and the limits are not competitive with those from e^+e^- colliders. In Sec. 4 we discuss the implications for a real-time experiment like Borexino which is aimed to detect ${}^7\text{Be}$ neutrinos. Finally, in Sec. 5 we summarise our findings.

2 Neutrino non-standard interactions

In the Standard Model, the elastic scattering $\nu e \rightarrow \nu e$ is described at low energy by the following (flavour conserving) four-fermion operator ($\nu = \nu_e, \nu_\mu, \nu_\tau$):

$$\mathcal{L}_{SM} = -2\sqrt{2}G_F(\bar{\nu}\gamma^\mu P_L\nu) [g_R(\bar{e}\gamma_\mu P_R e) + g_L(\bar{e}\gamma_\mu P_L e)], \quad (2)$$

where G_F is the Fermi constant, $P_{L,R} = (1 \mp \gamma^5)/2$ are the chiral projectors, and

$$g_L = \pm \frac{1}{2} + \sin^2 \theta_W, \quad g_R = \sin^2 \theta_W, \quad (3)$$

where in g_L the upper sign applies for ν_e and the lower one for $\nu_{\mu,\tau}$. An equivalent expression for the Lagrangian (2) is that in terms of the vector and axial electron current, i.e.

$$\begin{aligned} \mathcal{L}_{SM} &= -\sqrt{2}G_F(\bar{\nu}\gamma^\mu P_L\nu) [g_V(\bar{e}\gamma_\mu e) - g_A(\bar{e}\gamma_\mu \gamma_5 e)], \\ g_V &= g_R + g_L, \quad g_A = g_L - g_R. \end{aligned} \quad (4)$$

We assume on phenomenological grounds that neutrinos have NS weak-strength interactions with the electron described by the following four-fermion operator:

$$\mathcal{L}_{eff} = -2\sqrt{2}G_F(\bar{\nu}\gamma^\mu P_L\nu) [\varepsilon_R(\bar{e}\gamma_\mu P_R e) + \varepsilon_L(\bar{e}\gamma_\mu P_L e)], \quad (5)$$

Here ε_R and ε_L parameterize the strength of the new interactions with respect to the Fermi constant G_F . This entails a redefinition of the NC coupling constants g_L, g_R for $\nu e \rightarrow \nu e$ reaction, as

$$g_R \rightarrow g_R + \varepsilon_R, \quad g_L \rightarrow g_L + \varepsilon_L. \quad (6)$$

Novel interactions (5) can in general be flavour conserving, though not flavour universal, as well as flavour changing. In the following we focus on the NS flavour conserving case. Therefore for different neutrinos, in (5) distinct effective NS couplings are to be understood $\varepsilon_{eR}, \varepsilon_{eL}, \varepsilon_{\mu R}, \varepsilon_{\mu L} \dots$ (When necessary, the flavour index will be restored.)

In a similar way, we also define the vector and axial coupling constants of the non-standard interactions, i.e. $\varepsilon_V = \varepsilon_R + \varepsilon_L$ and $\varepsilon_A = \varepsilon_L - \varepsilon_R$, and, correspondingly, g_A, g_V get similarly redefined, $g_{A(V)} \rightarrow g_{A(V)} + \varepsilon_{A(V)}$.

The neutrino non-standard interactions (5), due to $SU(2)_W \times U(1)_Y$ -invariance, in general emerge together with other interactions involving the related $S(2)_W$ -partners [15] (for more details and a more model independent approach see [13]):

$$-2\sqrt{2}G_F\kappa_{\tau R}(\bar{\tau}\gamma^\mu P_L\tau)(\bar{e}\gamma_\mu P_R e) + (\tau \rightarrow \mu) + (\tau \rightarrow e),$$

$$\begin{aligned}
& -2\sqrt{2}G_F\kappa_{\tau L}(\bar{\tau}\gamma^\mu P_L\tau)(\bar{e}\gamma_\mu P_L e) + (\tau \rightarrow \mu) + (\tau \rightarrow e), \\
& -2\sqrt{2}G_F[\zeta_{\tau L}(\bar{\nu}_\tau\gamma^\mu P_L\tau)(\bar{e}\gamma_\mu P_L\nu_e) + \text{h.c.}] + (\tau \rightarrow \mu), \\
& -2\sqrt{2}G_F(\bar{\nu}_e\gamma_\mu P_L\nu_e)[\xi_{\tau L}(\bar{\tau}\gamma^\mu P_L\tau) + \xi_{\nu_\tau L}(\bar{\nu}_\tau\gamma^\mu P_L\nu_\tau)] + (\tau \rightarrow \mu), \\
& -2\sqrt{2}G_F\xi_{\nu_e L}(\bar{\nu}_e\gamma_\mu P_L\nu_e)(\bar{\nu}_e\gamma_\mu P_L\nu_e),
\end{aligned} \tag{7}$$

where, the various dimensionless parameters $\kappa_{\alpha R}, \kappa_{\alpha L}, \dots$ are also in general different from $\varepsilon_{\alpha R}, \varepsilon_{\alpha L}$ in (5) because of $SU(2)_W$ -breaking effects [15, 13].

Now we have to recall the existing limits on NS interactions. In the following we shall disregard the second-generation doublet since non-standard interactions of either ν_μ or μ with electrons are already severely bounded and then they would not be relevant in the next discussion. We notice that the interactions (7) governed by the parameters ξ_α and ξ_{ν_α} are unobservable and as such are unconstrained. Only the $\kappa_{\alpha R}, \kappa_{\alpha L}, \zeta_{\alpha L}$ -like interactions are phenomenologically testable and, indeed, there exist bounds on the associated couplings. The most stringent constraints on the $\kappa_{\alpha R}, \kappa_{\alpha L}$ -like interactions are derived from the collisions $e^+e^- \rightarrow e^+e^-$ and $e^+e^- \rightarrow \tau^+\tau^-$ at LEP [16], namely (at 95% C.L.):

$$\begin{aligned}
\kappa_{eR} &\lesssim 0.01, & \kappa_{eL} &\lesssim 0.03, \\
\kappa_{\tau R} &\lesssim 0.1, & \kappa_{\tau L} &\lesssim 0.02.
\end{aligned} \tag{8}$$

On the other hand, the strongest bound on the third-generation is that on the ζ_τ -interaction (7) from the decay $\tau \rightarrow e\nu_\tau\bar{\nu}_e$ [16]:

$$|\zeta_{\tau L}| \lesssim 0.003. \tag{9}$$

As for the neutrino non-standard interactions (5) the most stringent bounds have been recently derived from the measurement of $e^+e^- \rightarrow \nu\bar{\nu}\gamma$ cross section at LEP (for more details see [13]). We find for ν_e at 99% C.L.:

$$\begin{aligned}
-1.5 &\leq \varepsilon_{eL} \leq 0.2, & (\text{any } \varepsilon_{eR}), \\
-0.75 &\leq \varepsilon_{eR} \leq 0.85, & (\text{any } \varepsilon_{eL}), \\
-1.7 &\leq \varepsilon_{eV} \leq 0.7, & (\text{any } \varepsilon_{eA}), \\
-1.9 &\leq \varepsilon_{eA} \leq 0.5, & (\text{any } \varepsilon_{eV})
\end{aligned} \tag{10}$$

and for ν_τ

$$\begin{aligned}
-0.68 &\leq \varepsilon_{\tau L} \leq 0.45, & (\text{any } \varepsilon_{\tau R}), \\
-0.45 &\leq \varepsilon_{\tau R} \leq 0.62, & (\text{any } \varepsilon_{\tau L}), \\
-0.82 &\leq \varepsilon_{\tau V} \leq 0.70, & (\text{any } \varepsilon_{\tau A}), \\
-1 &\leq \varepsilon_{\tau A} \leq 0.55, & (\text{any } \varepsilon_{\tau V}).
\end{aligned} \tag{11}$$

The comparison between the bounds in eqs. (8-9) and those in eqs.(10-11) shows that the most severe laboratory bounds rather apply to the $SU(2)_W$ doublet partner of ν_τ and ν_e . Novel interactions of ν_τ, ν_e may have strength nearly close to the familiar Fermi interaction. From a theoretical point of view, the strong bounds on the $\kappa_{\alpha R(L)}, \zeta_{\alpha L}$ -interactions would directly apply also to the neutrino interactions (5). However, this is not necessarily true, because sizeable $SU(2)_W$ -breaking effects can spoil the $SU(2)_W$ -relationship among those parameters [15, 13].

Finally, we would like to mention that phenomenological bounds on NS flavour-changing as well as flavour-diagonal neutrino interactions have been recently obtained by atmospheric neutrino data fitting [17]. However, these bounds apply to the NS vector-coupling $\varepsilon_{\tau V}$. For

the flavour-diagonal coupling with electrons (denoted as ε'_e by the authors of [17]) we have inferred that $\varepsilon_{\tau V} \lesssim 0.2$ at 99% C.L.. More conservative estimates can be deduced from the atmospheric neutrino analysis performed in [18]. There, the bound obtained on the amount $\sin^2 \xi$ of sterile neutrino mixed with ν_τ , $\sin^2 \xi < 0.8$, can be translated into $\varepsilon_{\tau V} \lesssim 0.4$ at 90% C.L.. However, these analyses do not rule out the pure sterile oscillation which would imply $\varepsilon_{\tau V} \lesssim 0.5$ at 90% C.L.. Thereby, in the following we prefer to keep an open mind and consider $\varepsilon_{\alpha R}, \varepsilon_{\alpha L}$, ($\alpha = e, \tau$) to be order one as the bounds (10, 11) indicate.

2.1 Solar ν detection and NS interactions

Now let us turn to the relevance of these extra interactions for the solar neutrino detection via the elastic scattering off electrons, $\nu e^- \rightarrow \nu e^-$. The original solar neutrino distribution can be reproduced from the measurement of the recoil electron energy spectrum:¹

$$S(T) = \sum_i \int dE \lambda_i(E) \phi_i \left[P(E) \frac{d\tilde{\sigma}_{\nu_e}(E, T)}{dT} + (1 - P(E)) \left(c_{23}^2 \frac{d\tilde{\sigma}_{\nu_\mu}(E, T)}{dT} + s_{23}^2 \frac{d\tilde{\sigma}_{\nu_\tau}(E, T)}{dT} \right) \right]. \quad (12)$$

The differential cross sections are ($\alpha = e, \mu, \tau$):

$$\frac{d\tilde{\sigma}_{\nu_\alpha}(E, T)}{dT} = \int_0^{T'_{max}} dT' \frac{2G_F^2 m_e}{\pi} \left[g_L^2 + g_R^2 \left(1 - \frac{T'}{E}\right)^2 - g_L g_R \frac{m_e T'}{E^2} \right] \rho(T, T'), \quad (13)$$

where T is the ‘reconstructed’ recoil electron kinetic energy, while T' is the ‘true’ value as given by the kinematics and ranging as $0 \leq T' \leq T'_{max}$ with $T'_{max} = \frac{E}{1+m_e/2E}$ and $\rho(T, T')$ is the resolution function (explicitly given below). ϕ_i are the fluxes of all the solar neutrino sources contributing to the signal ($i = {}^8\text{B}$, ${}^7\text{Be}$, pp etc.), $\lambda_i(E)$ are the corresponding energy spectra (normalized to unity) and $P(E)$ is the generic ν_e survival probability.² Finally, non-standard interactions can be included according to the re-definition of the coupling constants g_L, g_R shown in eq. (6). From eq. (12) we notice the advantage of using monochromatic neutrinos, such as ${}^7\text{Be}$, since in this case the smearing on the electron distribution due to the integration over the neutrino energy is absent. Then in this case, even if neutrino conversions can change substantially the global rate, the energy distribution in the SM scenario ($\varepsilon_{\alpha R}, \varepsilon_{\alpha L} = 0$) does not get substantially deformed in shape. Therefore, for mono-energetic neutrinos a distortion of the electron energy distribution would be an unambiguous evidence of neutrino non-standard interactions. This would represent a unique signature of new physics that may be provided by solar neutrino experiments.

3 SNO *versus* Super Kamiokande

The SNO and SK experiments are both sensitive only to the ${}^8\text{B}$ neutrinos (except for the smaller *hep* neutrino flux). The SNO experiment detects solar neutrinos with most significance

¹ In the evaluation of the energy spectra $S(T)$ we take into account radiative corrections [19].

² As the neutrino fluxes ϕ_i and the probability $P(E)$ depend on the distance from the Sun and the Earth, it is understood an average over the time period.

via the CC reaction $\nu_e d \rightarrow p p e^-$ that is sensitive only to the ν_e flavour, while SK uses $\nu_\alpha e^- \rightarrow \nu_\alpha e^-$ scattering which is sensitive to all flavours, though the sensitivity to $\nu_{\mu,\tau}$ is a factor 6 smaller. The measured fluxes normalized to the SSM predictions [20] are:

$$Z_{SK} = 0.459 \pm 0.017, \quad Z_{SNO} = 0.347 \pm 0.027 \quad (14)$$

from where we infer that the relative gap between the two signals may be filled by $\nu_{\mu,\tau}$ -induced events in SK due to the solar neutrino conversion $\nu_e \rightarrow \nu_a$. This is the feature which makes the ν_e depletion into sterile neutrinos less plausible. For the sake of completeness, below we shall also consider the conversion of solar neutrinos into a combination of active and sterile state.

To discuss the impact of the NS interactions we take the following point of view. First, in view of the absence of a significant energy spectral deformation as reported by both SK and SNO experiments, we assume that the ν_e survival probability P be a constant, i.e. energy independent factor, at least in the energy range explored by SK and SNO ($E \geq 5$ MeV). Second, as the 8B flux is determined by SSM with an accuracy of 20% or so we treat it as a free parameter parameterized by f_B , i.e. as $f_B \cdot \phi_B$. Then experimental results can be expressed as follows:

$$Z_{SNO} = f_B \cdot P, \\ Z_{SK} = f_B \left[P \frac{R_e(\varepsilon_{eR}, \varepsilon_{eL})}{R_e^{SM}} + s_{as}^2 (1 - P) \frac{R_\mu^{SM}}{R_e^{SM}} \cdot \left(c_{23}^2 + s_{23}^2 \frac{R_\tau(\varepsilon_{\tau R}, \varepsilon_{\tau L})}{R_\mu^{SM}} \right) \right]. \quad (15)$$

The expression for Z_{SK} is quite general as it can account for the case of partial sterile conversion, $\nu_e \rightarrow s_{as}\nu_a + c_{as}\nu_s$ through the parameter s_{as}^2 that measures the fraction of solar ν_e 's that are converted into active neutrinos ($s_{as} = \sin \theta_{as}$, $c_{as} = \cos \theta_{as}$).³ The case $s_{as} = 1$ corresponds to the two-generation $\nu_e \rightarrow \nu_a$ (fully active) conversion, whereas $s_{as} = 0$ corresponds to the two-generation $\nu_e \rightarrow \nu_s$ (fully sterile) conversion. The 'spectral' functions R_α given by:

$$R_\alpha = \int dE \lambda(E) \tilde{\sigma}_{\nu_\alpha}, \quad \tilde{\sigma}_{\nu_\alpha} = \int_{T_{th}}^{T_{max}} dT \frac{d\tilde{\sigma}_{\nu_\alpha}(E, T)}{dT} \quad (16)$$

are understood to include also the contributions from neutrino NS interactions. By the notation R_α^{SM} ($\alpha = e, \mu, \tau$) we mean the same function when the NS couplings are set to zero and the SM expression is so recovered. The resolution function accounted in $\tilde{\sigma}_{\nu_\alpha}$ is

$$\rho(T, T') = \frac{1}{\sqrt{2\pi}\sigma} \exp \left[-\frac{(T - T')^2}{2\sigma^2} \right], \quad \sigma = \sigma_0 \sqrt{\frac{T'}{\text{MeV}}}, \quad (17)$$

where $\sigma_0 = 0.47$ MeV for Super Kamiokande, and the 'reconstructed' kinetic energy T ranges between the threshold value $T_{th} = (5 \text{ MeV} - m_e)$ and $T_{max} = (20 \text{ MeV} - m_e)$.

3.1 The active-sterile conversion

First we have analysed the conversion $\nu_e \rightarrow s_{as}\nu_a + c_{as}\nu_s$, where for the time being ν_e and ν_τ are assumed to have only SM interactions so that in Eq. (15) the Super Kamiokande signal gets simplified into

$$Z_{SK} = f_B \left[P + s_{as}^2 (1 - P) \cdot \frac{R_\mu^{SM}}{R_e^{SM}} \right], \quad (18)$$

³ For recent analysis of solar neutrino data in the context of four-neutrino scheme see e.g. [18, 21].

where $R_\mu^{SM}/R_e^{SM} \approx 0.16$ (for the electron energy threshold $E_e = 5$ MeV). The SNO and SK signals depend on the parameters f_B (or P) and s_{as} . So upon comparing the two signals we can constrain the Boron flux, i.e. the parameter f_B and the active-fraction parameter s_{as} . In Fig. 1 we have shown the allowed $1-\sigma$ region in the plane (f_B, s_{as}^2) (left panel). As we could expect, the asymptotic regime of large flux normalization f_B does not let s_{as} be vanishing and then the pure sterile conversion is strongly disfavoured. For the ‘central value’ of the Boron flux ($f_B = 1$) we find $s_{as}^2 \geq 0.7$, while within the SSM uncertainty, $f_B = 0.84 - 1.2$ (enclosed by the dashed vertical lines), $s_{as}^2 \geq 0.5$.⁴ As for the ν_e survival probability, the SSM range of f_B implies that $0.32 \lesssim P \lesssim 0.38$ (at $1-\sigma$). The same exercise has been repeated by allowing only ν_τ to have non-standard interactions. Now we have to refer to the more general expression for Z_K displayed in Eq. (15). Hence the ratio of the effective ν_τ cross section with that of ν_μ (which is given only by SM interactions), $r_\tau = R_\tau/R_\mu^{SM}$, is the extra parameter involved in this more general scenario. In Fig. 1 we have shown in the plane (r_τ, s_{as}^2) (right panel) the $1-\sigma$ allowed region for different values of the flux normalization, $f_B = 0.84, 1, 1.2$ which should account for the SSM uncertainty. The larger is the ν_τ cross section, $r_\tau > 1$, the larger is the fraction of solar neutrinos that can be converted into a sterile state with respect to the SM case ($r_\tau = 1$). Nevertheless, at $1-\sigma$ the pure sterile conversion cannot be reached even for $r_\tau \sim 3 - 4$. For the sake of comparison, we can see that, for instance with $f_B = 1$, the fraction of ν_e converted into ν_s varies from $\sim 30\%$ for $r_\tau = 1$ to $\sim 68\%$ for $r_\tau \sim 3$. Similar exercise has been done by allowing only ν_e to have NS couplings (see Fig. 2). We can observe the different shape of the iso-contours in Fig. 1 (right panel) with those in Fig. 2. As the ν_e contribution to the Z_{SK} signal dominates over that of ν_μ, ν_τ , now by increasing the ν_e cross section, $r_e \sim 1.25 - 1.5$, the conversion could be completely sterile ($s_{as} = 0$). Notice that all the curves in Fig. 2, corresponding to three different values of f_B , are attracted to the ‘fixed’ range $r_e = 1.25 - 1.5$ for $s_{as}^2 = 0$, since the Z_{SK} signal becomes $Z_{SK} = r_e \cdot Z_{SNO}$. However, we will see below that this possibility is disfavoured because such large ν_e cross section is in contradiction with e^+e^- collider data.

Clearly, this three-parameter analysis is insufficient to constrain neutrino NS interactions. To extract some information on neutrino NS interactions in the next Section we consider in more detail the pure active conversion $\nu_e \rightarrow \nu_a$ (fixing in this way one parameter, $s_{as}^2 = 1$).

3.2 NS interactions and pure active conversion

We have performed the same analysis done in the previous section for the solar neutrino conversion into the active combination ν_a of ν_μ and ν_τ , $\nu_a = (\nu_\mu - \nu_\tau)/\sqrt{2}$. Therefore in the expression for the SK signal in (15) we have set $s_{as} = 1$. First, we consider the case with NS interactions of ν_τ . The results are shown in Fig. 3 (left panel). In this case, for large enough Boron flux, $f_B \gtrsim 1.2$, the ν_τ is allowed to become ‘sterile’ i.e. r_τ could go to zero as the SK signal would be recovered by the ν_μ active portion. On the contrary, for $f_B < 1.4$ the ν_τ cross section could be larger than the SM one. Then within the SSM prediction for f_B (delimited by dashed vertical lines) we find $0 \lesssim r_\tau \lesssim 3$. The same procedure has been applied for the case of NS interactions of ν_e and only SM interactions for ν_τ (see right panel in Fig. 3). We may notice that in this case, even for large value of f_B the ratio r_e cannot approach zero, since the ν_a contribution to the Z_{SK} signal is not enough, and the increase of r_e by decreasing f_B is

⁴Our allowed region somewhat differs from other analysis as that in [4] because of different ‘fitting’ procedure.

much more modest than in the case of NS interactions of ν_τ . Then in this case the ratio r_e is confined in a more narrow range, $0.85 \lesssim r_e \lesssim 1.25$, taking the SSM range of f_B . At this point, the allowed range for r_α ($\alpha = e, \tau$) can be read as allowed space for the parameters $\varepsilon_{\alpha R}, \varepsilon_{\alpha L}$ or, equivalently, for $\varepsilon_{\alpha A}, \varepsilon_{\alpha V}$. These are shown in Fig. 4 and Fig. 5, for ν_τ and ν_e , respectively.⁵ First, it is interesting to notice that $r_\alpha = 0$ corresponds in terms of $\varepsilon_{\alpha R}, \varepsilon_{\alpha L}$ to the single solution $\varepsilon_{\alpha R} = -g_R$, $\varepsilon_{\alpha L} = -g_L$. For example, for ν_τ this implies $\varepsilon_{\tau L} \approx -\varepsilon_{\tau R}$, thanks to the accidental fact that $\sin^2 \theta_W$ is close to $1/4$. In Fig. 4 and Fig. 5 (see left panels) we have drawn the $\varepsilon_{\tau L} = -\varepsilon_{\tau R}$ and $\varepsilon_{eL} = -\varepsilon_{eR}$ *locus*, respectively (solid line). Along this line, the vector neutral coupling $g_V = g_L + g_R$ is that of the SM. As a result, in the case illustrated in Fig. 4, ν_μ and ν_τ have the same forward scattering-amplitude off electrons and therefore they have the same matter potential. This implies no matter effects on the atmospheric $\nu_\mu \rightarrow \nu_\tau$ (vacuum) oscillation pattern. In conclusion, the points on this line cannot be tested by atmospheric neutrino experiments. For an easier reading in the right panel of Fig. 4 we have delimited by solid horizontal lines the region $|\varepsilon_V| \lesssim 0.5$ constrained by atmospheric neutrino data (at 90% C.L.) [18, 17]. Then, we learn that the range $r_\tau \lesssim 3$, inferred for ν_τ NS interactions, imply most conservatively, i.e. ignoring any correlation, the following limits (at $1\text{-}\sigma$)

$$\begin{aligned}
-0.2 &\leq \varepsilon_{\tau L} \leq 0.7, & (\text{any } \varepsilon_{\tau R}), \\
-1.7 &\leq \varepsilon_{\tau R} \leq 1.3, & (\text{any } \varepsilon_{\tau L}), \\
-1.7 &\leq \varepsilon_{\tau V} \leq 1.7, & (\text{any } \varepsilon_{\tau A}), \\
-1.2 &\leq \varepsilon_{\tau A} \leq 2.1, & (\text{any } \varepsilon_{\tau V})
\end{aligned} \tag{19}$$

The comparison with (11) shows that solar neutrino experiments provide much less sensitivity to non-standard interactions. Analogously for the case of NS interactions of ν_e we find:

$$\begin{aligned}
-1.6 &\leq \varepsilon_{eL} \leq 0.1, & (\text{any } \varepsilon_{eR}), \\
-2.8 &\leq \varepsilon_{eR} \leq 2.3, & (\text{any } \varepsilon_{eL}), \\
-3.8 &\leq \varepsilon_{eV} \leq 1.8, & (\text{any } \varepsilon_{eA}), \\
-3.2 &\leq \varepsilon_{eA} \leq 2.2, & (\text{any } \varepsilon_{eV})
\end{aligned} \tag{20}$$

Also these bounds once confronted with those derived from LEP (10) are much more modest (notice also the different ‘confidence levels’ shown). Therefore, for example, the novel possibility of full sterile conversion with ν_e having ‘stronger’ than weak interactions, arisen from Fig. 2, would require a parameter space already excluded by e^+e^- collider limits.

At this point, we may wonder about the implications of NS interactions with electrons for the energy spectrum measured at SK (since in the previous analysis we consider only the global rate Z_{SK}). Without entering into a detailed analysis, which is beyond our scope, we have performed a scanning of the $(\varepsilon_{\tau R}, \varepsilon_{\tau L}, P)$ and $(\varepsilon_{eR}, \varepsilon_{eL}, P)$ space at time (fixing $f_B = 1$, for example) to fit the data of the SK spectrum. We have realized that both $\varepsilon_{\tau R}$ and ε_{eR} are poorly constrained, while $\varepsilon_{\tau L}$ is confined within $\sim (0 - 0.5)$ and $\varepsilon_{eL} \sim 0$ with $P \sim 0.3 - 0.4$.

In conclusion, we have learnt that neutrino NS interactions are not significantly constrained by solar neutrino data. In the next Section we shall investigate the Borexino capability in testing these neutrino extra interactions, taking into account the allowed parameter space for $(\varepsilon_{\alpha R}, \varepsilon_{\alpha L})$ [13].

⁵ Though the information content is redundant, we have shown the parameter space for both $\varepsilon_{\alpha R}, \varepsilon_{\alpha L}$ and $\varepsilon_{\alpha A}, \varepsilon_{\alpha V}$. Perhaps, the former parameterization would be preferred by ‘model builders’ and the latter by ‘neutrino phenomenologists’.

4 Analysis for Borexino detector

We consider as prototype for our discussion the Borexino experiment which is aimed to detect monochromatic ${}^7\text{Be}$ neutrinos via ν - e elastic scattering [22]. The beryllium neutrino flux can be measured by exploring the energy window $T = 0.25 - 0.66$ MeV for the recoil electron: 0.25 is the attainable detection threshold and 0.66 is the Compton edge. In this window, 80% of the signal is from the ${}^7\text{Be}$ neutrinos, while the rest comes from the CNO and pep neutrinos. In fact, both the edges get smeared when the energy resolution is taken into account and the lower part of the spectrum is arisen by the pp and ${}^7\text{Be}(0.38\text{MeV})$ neutrinos. This feature is clearly apparent in Fig. 6 where the energy distributions of the expected events in Borexino are plotted. The resolution function used is of the form in Eq. (17) with width $\sigma_0 = 57.7$ KeV [23]. In Fig. 6 the solid line gives the SSM energy distribution from all solar ν_e sources ($pp + {}^7\text{Be}(0.38, 0.86)\text{MeV} + \text{CNO} + pep$), while the contribution of only Beryllium neutrinos is shown by dotted line. The lowest curve represents the events distribution as expected if all ν_e 's were converted into the combination ν_a assuming for ν_μ, ν_τ only the standard model NC couplings ($\varepsilon_R, \varepsilon_L = 0$). In this case the distribution is flatter in the range (0.3-0.6) MeV ($\Delta S(T)/S(T) \sim 14\%$).

Now let us turn to neutrino oscillations. The several scenarios proposed to explain the SNA predict different survival probabilities for the beryllium neutrinos. For example the suppression can be quite strong, $P \lesssim 20\%$ in case of small-mixing angle MSW conversion, but can be weaker, $P \sim 30 - 50\%$, in case of vacuum oscillation or large-mixing angle MSW conversion. On the other hand, as mentioned, neutrino conversions are expected not to distort the energy distribution as long as $\nu_{\mu,\tau}$ have only SM interactions. Then the energy spectrum will be just re-scaled with a slope which will be in between that of the SSM distribution and that expected in case of complete depletion of solar ν_e (lower dashed curve in Fig. 6).

We discuss now how this picture gets modified when NS interactions of neutrinos are switched on. The plots gathered in Fig. 7 represent the expected event distribution at Borexino as a result of $\nu_e \rightarrow (\nu_\mu - \nu_\tau)/\sqrt{2}$ transition for some points in the plane $(\varepsilon_{\tau R}, \varepsilon_{\tau L})$ and $(\varepsilon_{e R}, \varepsilon_{e L})$, compatible (or, in certain case, marginally compatible) with the existing bounds. In each of the figures (b), (c), (d) we have considered for the same pair of NS couplings, both the case in which only ν_τ has non-standard interactions (and ν_e, ν_μ have only SM interactions) (solid lines) and that in which only ν_e has non-standard interactions (dotted lines). Each case has been considered for two values of the survival probability, i.e. $P = 0.5$ (upper lines) and $P = 0.35$ (lower lines). For the sake of comparison in the panel (a) we have illustrated also the case in which all neutrino flavours have only SM interactions $(\varepsilon_{\alpha R}, \varepsilon_{\alpha L}) = (0, 0)$ ($\alpha = e, \mu, \tau$). The two values used for P are in the range predicted for the ${}^7\text{Be}$ neutrinos by the large-mixing angle or low- δm^2 MSW solutions, which both provide a good description of the data [2], [4]. We can observe that the distortion of the shape is mostly due to the coupling ε_R (see figure (b)) contributing to g_R that controls the most T -dependent terms in the differential cross section. The effect is more dramatic for positive value of ε_R and vanishing ε_L : in Fig. 7 (b) we can see that the increase of the coupling g_R has provided a stronger variation of the spectrum with T and a more noticeable ‘negative’ slope. We also observe that the case in which only ν_e NS couplings are switched on can be distinguished by the one in which only ν_τ NS couplings are on. In the former case the decreasing of the spectrum is even sharper. The presence of the background in the lower-energy end may render hard to observe the part mostly deformed.

However, due to the exponential decay of the background⁶ it is still possible to reveal the deformation above (0.4 - 0.45) MeV. This strong deformation is attenuated as soon as the parameter ε_L is switched on (see Fig. 7 (c) and (d)). For example the case presented in figure (c) does not exhibit any deformation but for only $((\varepsilon_{\tau R}, \varepsilon_{\tau L}) = (0, -1))$ the total number of events with respect to the SM case (a) is nearly a factor three larger. On the other hand, for $(\varepsilon_{eR}, \varepsilon_{eL}) = (0, -1)$ (notice that now g_L is the same for ν_e and $\nu_{\mu, \tau}$) the spectrum is strongly depressed. We may wonder whether it is possible to invert the slope of the distribution in order to make it raise in the high energy part. This would require to satisfy the following relation:

$$\frac{T}{E} > 1 + \left(\frac{g_L}{g_R} \right) \frac{m_e}{2E}, \quad (21)$$

that, for example with ν_τ extra interactions, suggests to get more negative g_L and smaller g_R . The diminishing of g_R (with $\varepsilon_{\tau R} \sim 0.2$) suppresses the terms dependent on T and the overall effect of deformation is however weakened even for $\varepsilon_{\tau L} \lesssim -1$. Then, at least within the allowed parameter space of the NS couplings, we have not found examples in which the slope gets positive.⁷

Now we would like to face a more future issue related to future low-energy neutrino experiments. For the sake of simplicity and brevity, we take into account only ${}^7\text{Be}$ neutrinos. (In particular we want to get rid of the continuous pp flux and therefore the energy window $T = 0.3 - 0.6$ MeV should be taken.) This corresponds to consider the following function, normalized to the SSM expectation:

$$F(T) \equiv \frac{S(T)/S^0(T)}{(1-P)} - \frac{P}{(1-P)} = \frac{c_{23}^2 \frac{d\tilde{\sigma}_{\nu_\mu}(E, T)}{dT} + s_{23}^2 \frac{d\tilde{\sigma}_{\nu_\tau}(E, T)}{dT}}{\frac{d\tilde{\sigma}_{\nu_e}(E, T)}{dT}} \quad (22)$$

where $S^0(T)$ is the SSM energy spectrum expected in Borexino. This observable $F(T)$ can be in fact built up by subtracting from the energy distribution $S(T)$ measured at Borexino the ν_e survived contribution as ‘directly’ measured by a low-energy neutrino experiment such as LENS – sensitive *only* to the ν_e flavour [25]. In this way we would more directly test the ν_μ, ν_τ contribution to the energy distribution. This complementary role between these two kinds of experiments is analogous to that presently played by Super-Kamiokande and SNO for the high-energy ${}^8\text{B}$ neutrinos.

5 Conclusions

Extensions of the Standard Model generally include new neutral current interactions that can be flavour changing as well as flavour conserving. It is interesting that very recently the NuTeV results on the determination of electroweak parameters show a discrepancy with the SM expectation that suggests non-standard couplings of neutrinos with quarks [26].

⁶The shape of the background increases from 0.25 up to 0.4 MeV and for $T \gtrsim 0.4$ MeV exponentially decay; this can be found for example in Fig. 2 in [24].

⁷ Notice that even if parametrically this can be achieved for, say, the ${}^7\text{Be}$ -line, the inclusion all neutrino sources and of the resolution function (17) spoils the effect.

In this paper, we have re-examined the implications for solar neutrino detection of non-standard flavour conserving interactions of neutrinos with electrons. In particular, we have paid special attention to the case in which ν_τ and ν_e have non-standard couplings with electrons. In the light of the atmospheric neutrino data pointing to a large mixing between ν_μ and ν_τ , the solar neutrino deficit can now be regarded as the ‘conversion’ of $\sim 65\%$ of solar ν_e ’s into an equal amount of ν_μ and ν_τ . We have found that present solar neutrino experiments do not show a better sensitivity to such novel interactions with respect to that achieved by e^+e^- collider. We have so tried to reverse the point of view by looking for some signature of such NS interactions within the allowed parameter space. We have demonstrated that the allowed range for these neutrino non-standard interactions could be tested by Borexino experiment, aimed to detect the monochromatic ${}^7\text{Be}$ -line. Indeed, neutrino NS interactions could manifest especially through an unexpected spectral deformation and in most cases with an ‘anomalous’ increase of the number of total events. Finally, we would like to comment about the possibility, which is usually neglected, to solve the solar neutrino deficit with matter oscillations induced by flavour-changing and flavour-conserving NS interactions of neutrinos with electrons (with massless neutrinos) [9]. Indeed, also such flavour-changing NS interactions (the relevant flavour-changing parameters would be $\varepsilon_{e\beta V}$, $\beta = \mu, \tau$) are not strongly constrained [13] and, jointly with the flavour-diagonal NS ones, can give rise to a sizeable mixing angle in matter. Therefore, it could be worth re-considering such conversion mechanism.

Acknowledgments We would like to thank Luca Girlanda and Paolo Ronchese for ‘graphics’ assistance.

References

- [1] C. McGrew [Super-Kamiokande Collaboration], talk given at 9th International Workshop on ‘Neutrino Telescopes’, 6-9 March 2001, Venice, Italy; Transparencies available at <http://axpd24.pd.infn.it/conference2001/venice01.html>.
- [2] For a recent review, see for example: M. C. Gonzalez-Garcia, M. Maltoni, C. Pena-Garay and J. W. Valle, Phys. Rev. D **63** (2001) 033005;
G. L. Fogli, E. Lisi, A. Marrone, D. Montanino and A. Palazzo, hep-ph/0104221.
- [3] In the SNO home page at: <http://www.sno.phy.queensu.ca/>
- [4] V. Barger, D. Marfatia and K. Whisnant, hep-ph/0106207;
J. N. Bahcall, M. C. Gonzalez-Garcia and C. Pena-Garay, hep-ph/0106258;
P. I. Krastev and A. Y. Smirnov, hep-ph/0108177
- [5] M. Apollonio *et al.* [CHOOZ Collaboration], Phys. Lett. B **466** (1999) 415.
- [6] Z. Berezhiani and A. Rossi, Phys. Rev. D **51** (1995) 5229.
- [7] L. Wolfenstein, Phys. Rev. D **17** (1978) 2369;
J. W. Valle, Phys. Lett. B **199** (1987) 432;
E. Roulet, Phys. Rev. D **44** (1991) 935;
M. M. Guzzo, A. Masiero and S. T. Petcov, Phys. Lett. B **260** (1991) 154.

- [8] Z. G. Berezhiani and A. Rossi, Proc. of the 5th Int. Workshop on ‘Neutrino Telescopes’, p. 123-135, ed. by M. Baldo Ceolin, Venice, Italy, 1993; hep-ph/9306278; Nucl. Phys. Proc. Suppl. **35** (1994) 469.
- [9] V. Barger, R. J. Phillips and K. Whisnant, Phys. Rev. D **44** (1991) 1629.
- [10] S. Bergmann, M. M. Guzzo, P. C. de Holanda, P. I. Krastev and H. Nunokawa, Phys. Rev. D **62** (2000) 073001 and references therein.
- [11] S. P. Mikheev and A. Y. Smirnov, Nuovo Cim. C **9** (1986) 17;
L. Wolfenstein in [7].
- [12] J. N. Bahcall, N. Cabibbo and A. Yahil, Phys. Rev. Lett. **28** (1972) 316;
K. Tennakone and S. Pakvasa, Phys. Rev. D **6** (1972) 2494;
J. F. W. Valle, Phys. Lett. B **131** (1983) 87;
J. N. Bahcall, S. T. Petcov, S. Toshev and J. W. Valle, Phys. Lett. B **181** (1986) 369;
Z. G. Berezhiani and M. I. Vysotsky, *ibid.* **199** (1987) 281;
Z. G. Berezhiani, G. Fiorentini, M. Moretti and A. Rossi, Z. Phys. C **54** (1992) 581;
JETP Lett. **55** (1992) 151 [Pisma Zh. Eksp. Teor. Fiz. **55** (1992) 159].
- [13] Z. Berezhiani and A. Rossi, hep-ph/0111137.
- [14] M. Nakamura [DONUT Collaboration], Nucl. Phys. Proc. Suppl. **77** (1999) 259. B. Lundberg [DONUT Collaboration], Nucl. Phys. Proc. Suppl. **91** (2001) 233.
- [15] S. Bergmann, Y. Grossman and D. M. Pierce, Phys. Rev. D **61** (2000) 053005;
S. Bergmann *et al.* Phys. Rev. D **62** (2000) 073001.
- [16] D. E. Groom *et al.* [Particle Data Group Collaboration], Eur. Phys. J. C **15** (2000) 1.
- [17] N. Fornengo *et al.*, hep-ph/0108043.
- [18] G. L. Fogli, E. Lisi and A. Marrone, Phys. Rev. D **63** (2001) 053008; hep-ph/0105139.
- [19] J. N. Bahcall, M. Kamionkowski and A. Sirlin, Phys. Rev. D **51** (1995) 6146.
- [20] J. Bahcall, M. Pinsonneault and S. Basu, astro-ph/0010346. The ‘central value’ of the Boron and Beryllium fluxes are $\phi_B = 5.05 \times 10^6 \text{ cm}^{-2}\text{s}^{-1}$ and $\phi_{Be} = 4.77 \times 10^9 \text{ cm}^{-2}\text{s}^{-1}$, respectively.
- [21] C. Giunti, M. C. Gonzalez-Garcia and C. Pena-Garay, Phys. Rev. D **62** (2000) 013005;
O. Yasuda, hep-ph/0006319;
M. C. Gonzalez-Garcia, M. Maltoni and C. Pena-Garay, hep-ph/0105269.
- [22] C. Arpesella *et al.* [BOREXINO Collaboration], Proposal of Borexino, 1991 (unpublished);
G. Ranucci *et al.* [BOREXINO Collaboration], Nucl. Phys. Proc. Suppl. **91** (2001) 58.
- [23] G. Bellini [BOREXINO Collaboration], Nucl. Phys. Proc. Suppl. **48** (1996) 363.
- [24] E. Meroni [BOREXINO Collaboration], Nucl. Phys. Proc. Suppl. **100** (2001) 42.
- [25] R. S. Raghavan, Phys. Rev. Lett. **78**, 3618 (1997).
- [26] G. P. Zeller *et al.* [NuTeV Collaboration], hep-ex/0110059.

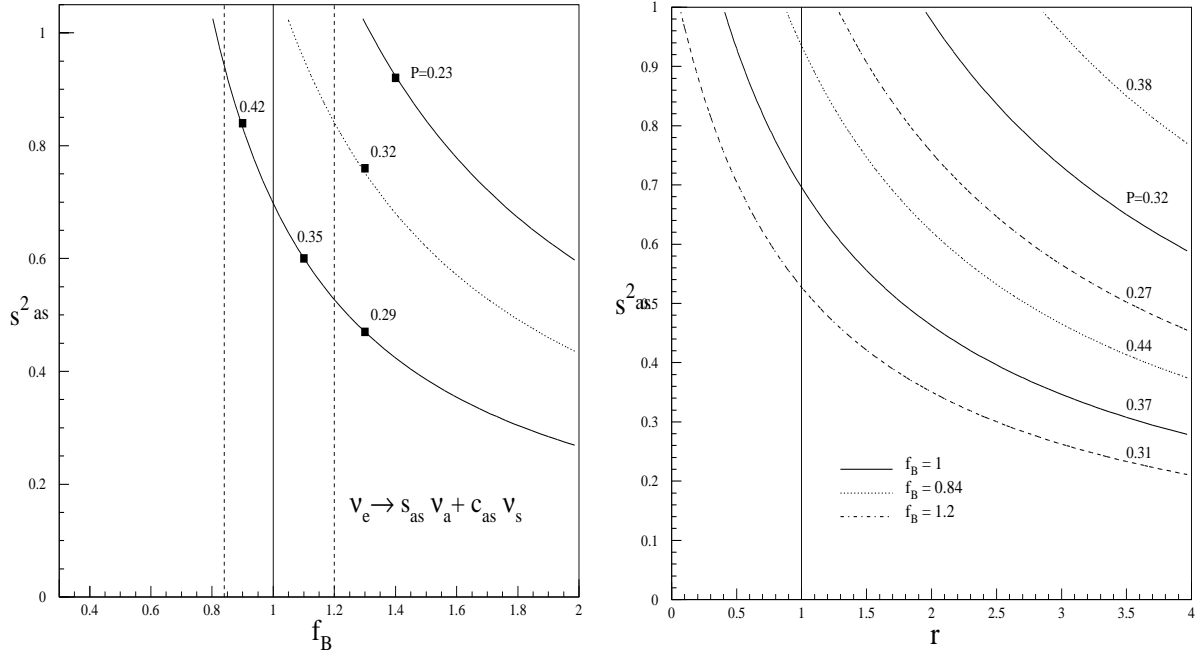


Figure 1: Analysis of SK and SNO assuming $\nu_e \rightarrow s_{as}\nu_a + c_{as}\nu_s$ conversion (ν_s is a sterile neutrino) in the plane scanned by the normalization factor f_B and s^2_{as} which is the fraction of the solar neutrinos converted into active neutrinos (right panel) and in the plane (r, s^2_{as}) (left panel) for given values of f_B . Here $r_\tau = R_\tau/R_\mu^{SM}$ is the ratio of the effective ν_τ elastic scattering cross section, including the NS interaction contribution, with the SM ν_μ cross section. The contours of the 1σ allowed region are shown by solid lines in the right panel (the dotted line in the middle refers to the central values of SK and SNO data). In the left panel the f_B range predicted by the SSM is shown by vertical dashed lines (for convenience we also show the $f_B = 1$ curve corresponding to the reference SSM model). As a guideline for the reader we have drawn (black squares) some points for the ν_e survival probability P which for given f_B is fixed by the SNO signal Z_{SNO} (see Eq. (15)).

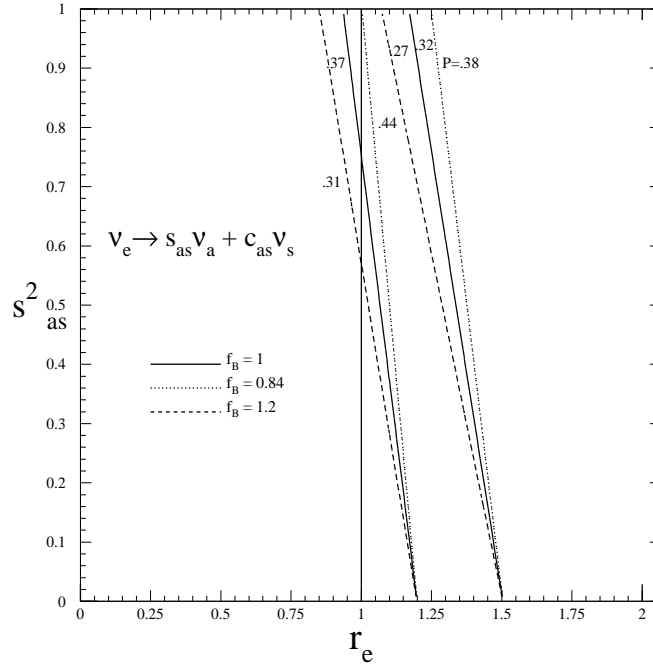


Figure 2: The same as in Fig. 1 (right panel) but in the plane (r_e, s^2_{as}) , where $r_e = R_e(\varepsilon_{eR}, \varepsilon_{eL})/R_e^{SM}$, i.e. now only ν_e is allowed to have NS interactions.

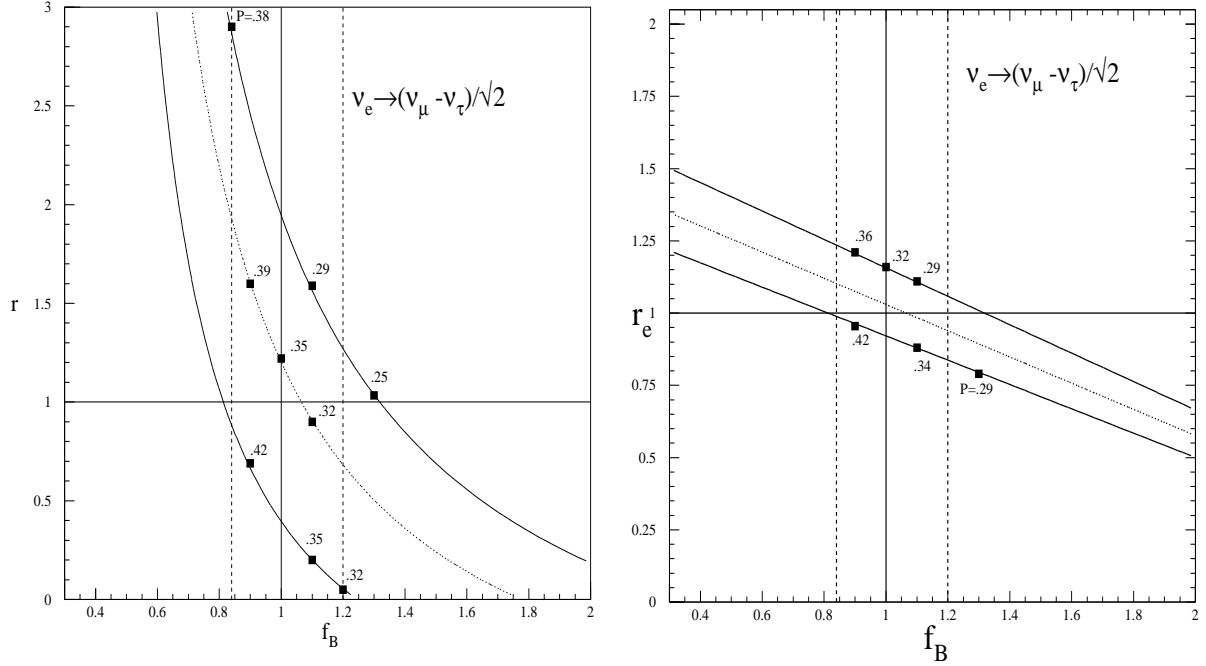


Figure 3: The same analysis as in Fig: 1 is performed for the conversion $\nu_e \rightarrow \nu_a = \frac{1}{\sqrt{2}}(\nu_\mu - \nu_\tau)$: In the left panel only the state ν_τ have non-standard interactions, and in the right panel only the state ν_e . The 1- σ allowed region in the plane (f_B, r) are delimited by solid lines.

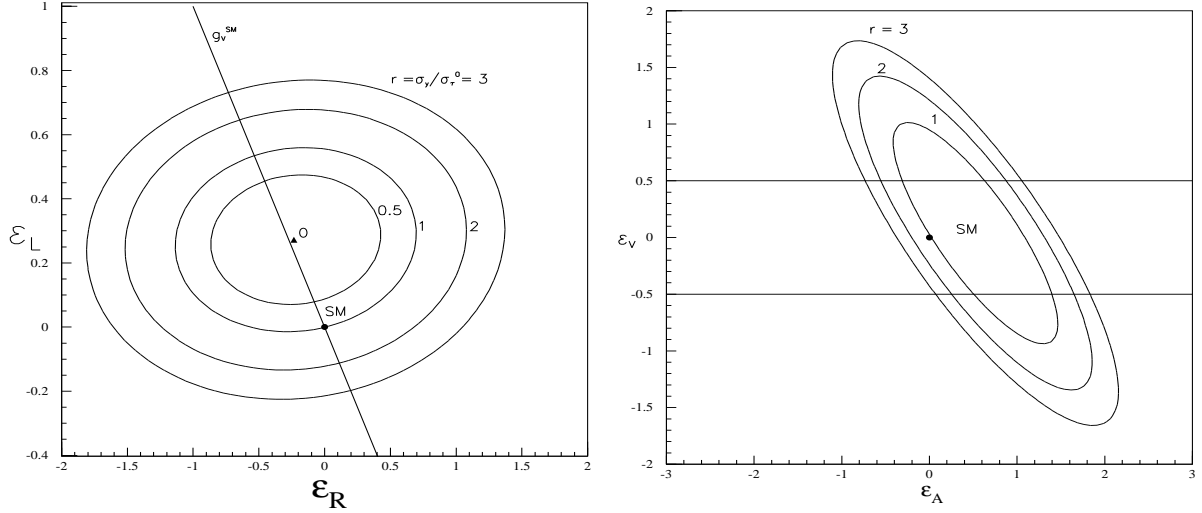


Figure 4: Here the information achieved from Fig: 3 on the allowed size of the ν_τ cross section is translated into allowed regions for the strength of NS interactions parameterised by $\varepsilon_{\tau R}, \varepsilon_{\tau L}$ (left panel) or by $\varepsilon_{\tau A}, \varepsilon_{\tau V}$ (left panel). The filled circle represents the Standard Model (SM) ν_τ cross section lying obviously on the contour $r_\tau = 1$. Notice that all other points on this curve would differentiate from the SM point by the shape of the differential cross section. The black triangle represents vanishing cross section. The solid line marked by g_V^{SM} singles out the points where $\varepsilon_{\tau L} = -\varepsilon_{\tau R}$ so that the vector coupling constant remains that of the SM ($\varepsilon_{\tau V} = 0$ -line in the right panel). The region limited by $|\varepsilon_{\tau V}| \leq 0.5$ is that allowed by atmospheric neutrino data.

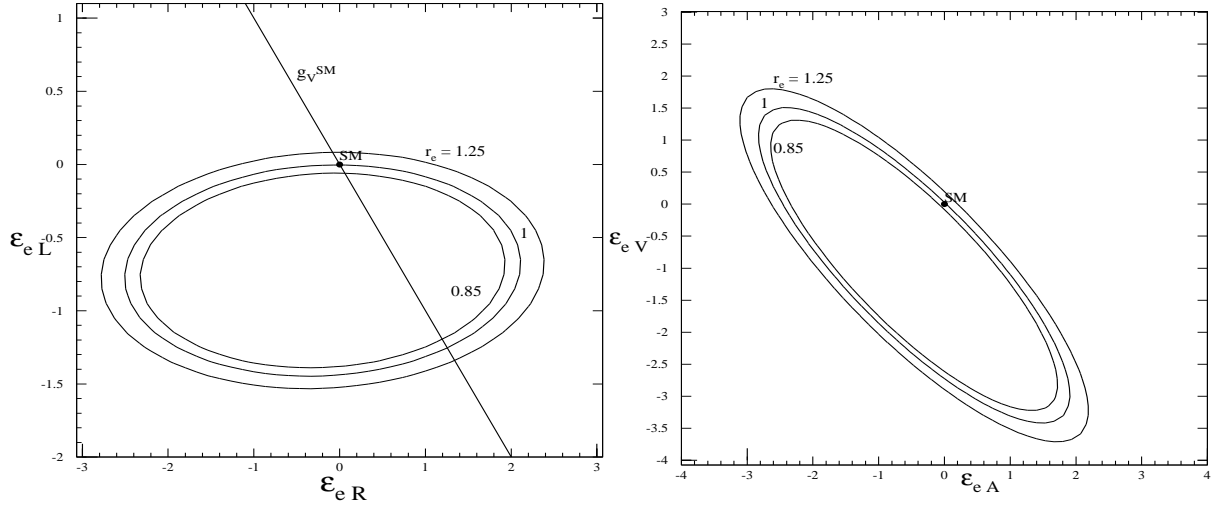


Figure 5: The same as in Fig. 4 but for the NS couplings of ν_e .

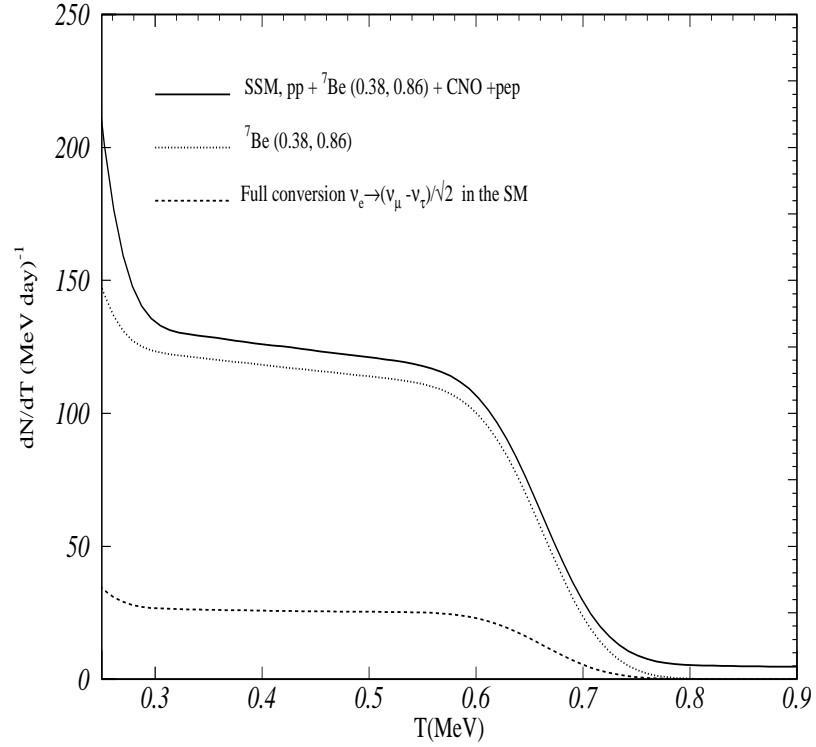


Figure 6: Energy distribution of the events expected in Borexino experiment in the relevant electron kinetic energy T . Only SM interactions are assumed. The solid line correspond to the distribution expected from the contribution of all relevant solar electron-neutrino sources ($pp, {}^7\text{Be}(0.38, 0.86\text{MeV}), \text{CNO}, \text{pep}$). For comparison we also show the distribution due to only the ${}^7\text{Be}(0.38, 0.86\text{MeV})$ neutrinos (dotted line). By assuming that all solar ν_e 's are converted into the combination $\nu_a = \frac{1}{\sqrt{2}}(\nu_\mu - \nu_\tau)$, the resulting spectrum is that drawn by the lower dashed curve. We observe that the slope gets less 'negative' compared to that predicted by the SSM.

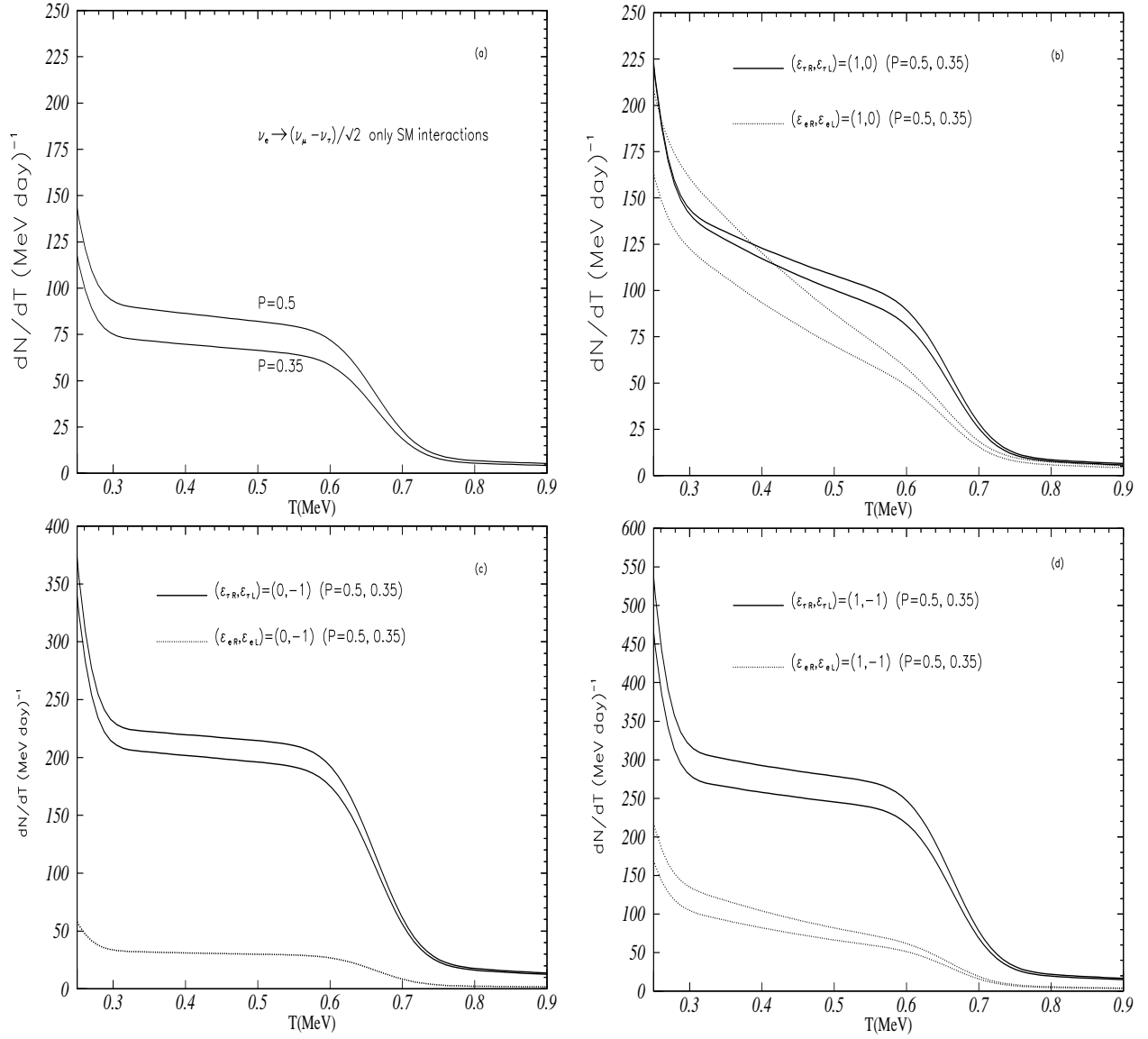


Figure 7: The expected event distribution at Borexino as a consequence of the active conversion $\nu_e \rightarrow (\nu_\mu - \nu_\tau)/\sqrt{2}$ for different values of NS couplings ($\varepsilon_{\alpha R}, \varepsilon_{\alpha L}$) ($\alpha = e, \tau$) as indicated in the figures. In figure (a) we show for comparison the energy distribution in case all neutrinos have only SM interactions ($\varepsilon_{\alpha R}, \varepsilon_{\alpha L} = (0, 0)$) for two values of the survival probability (energy independent): $P = 0.5$ (upper curve) and $P = 0.35$ (lower curve). In the panels (b),(c),(d) we put in comparison the distributions obtained when only ν_τ has NS couplings (solid lines) and when only ν_e has NS couplings (dotted lines). For each case, we considered, as in the panel (a), two values of P : $P = 0.5$ (upper curves) and $P = 0.35$ (lower curves). Notice that in figure (c), the curves for $P = 0.35$ and $P = 0.5$ are indistinguishable for the case when only ν_e has NS couplings.